Development of a Polymeric Optical Fiber Sensor for Stress Estimation: A Comparative Analysis between Physiological Sensors

María Gaitán-Padilla, Marcela Múnera, Maria José Pontes *Member, IEEE*, Marcelo Eduardo Vieira Segatto, Carlos A. Cifuentes *Senior Member, IEEE*, and Camilo A. R. Diaz *Member, IEEE*

***Abstract*— The global prevalence of stress and its far-reaching impact on well-being has spurred the pursuit of innovative solutions for physiological and stress monitoring. Existing methods, whereas informative, often lack cost-efficiency, daily usefulness, real-time capabilities, or user comfort. This study introduces a novel approach using a low-cost wearable polymeric optical fiber (POF) sensor to classify stress in 12 healthy individuals (seven women and five men) using the Trial Social Stress Test (TSST) method for stress induction. The study's methodology involves validating the POF sensor's physiological measurement, comparing it with a fiber Bragg Grating (FBG)-based sensor and with an electrocardiogram (ECG) commercial sensor, and subsequent making a stress classification approach using a Bagged Decision Tree Classifier (BDTC). To the authors' knowledge, this is the first work implementing POF and FBG sensors in stress detection. The results showcase the POF sensor's proficiency in capturing pulse and respiration signals, aligning closely with established monitoring sensors. The tested classification algorithm with the POF sensor exhibits an accuracy of 92.37% in the validation stage and 84.75%, recall of 79.41%, precision of 93.10%, and F-score of 85.71%. These results demonstrate the POF sensor's potential to be a reliable stress indicator. Also, considering the reduction in the size of the optical interrogation system for the POF sensor compared to FBG interrogation systems, the proposed sensor can be used in complete wearable systems. For future work, the sensor will be improved in terms of TRL and tested in real-scenario applications.**

***Index Terms*— Fiber Optic Sensors, Physiological Monitoring, Polymeric Optical Fiber, Stress Detection, Wearable**

I. Introduction

THE effects of stress on physical and mental health have been evaluated because it has been growing in the statistics of the World Health Organization (WHO), as well as the importance of stress management to avoid diseases related to the Autonomous Nervous System (ANS) [1]. In a significant sample of interviewed people in the United Kingdom, 74% felt so stressed they could not cope. As a behavioral result, 46% reported to be unhealthy and as psychological results, 51% reported depression and 61% anxiety [2]. Considering the physiological influence of stress on the body, the body's response to stressors has been studied by sensing parameters of the sympathetic system of the ANS. The ANS works in constant balance through the sympathetic and parasympathetic systems to maintain well-being, regulating breathing, heart control, digestive functions, and hormone release [3]. When stress occurs, hormones such as cortisol are released, saliva production stops, energy consumption is maintained by stopping digestive function, and cardiac function is highly regulated [4].

Therefore, it is helpful to monitor stress, which can assist adults and children in providing feedback, promoting stress management, and improving quality of life [5]. Nowadays, there are technologies for comprehending the behavior of the ANS [6]. Those sensors use different methods to estimate stress through physiological data. Through the number of hormones present in saliva [7], monitoring cardiac activity [8], and obtaining characteristics directly related to the regulation of the sympathetic system such as heart rate variability (HRV) [6]. Furthermore, respiratory sensors play a crucial role in monitoring breathing patterns and respiratory rates, as the measurement of other sympathetic responses like the use of galvanic skin response (GSR) sensors [9] reflecting changes in sweat gland activity. Some of these methods are not continuously monitorable [7], so the most effective method is by monitoring heart activity and HRV features.

The HRV is the variation in the time intervals between adjacent heartbeats; it is a validated method to detect stress due to cardiac regulations of the sympathetic system, which generates low and high-frequency variations [6]. Stress estimation with HRV relies on sensors to quantify changes in the body's responses [8]. Among the sensors employed in stress research are electrocardiograms (ECG), which record the heart's electrical activity, providing insights into HRV responses. Moreover, those sensors are costly and more oriented to clinical or research applications and not for everyday use. Another

This work is supported by FAPES (EXTRATO ATA DA 6ª REUNIÃO CCAF/2022 – "CPID 2.2"). Camilo A. R. Diaz acknowledges the financial support of FAPES (459/2021), CNPq (310668/2021-2), CNPq (404111/2023-8), and MCTI/FNDCT/FINEP (2784/20). This work was also supported by the UKRI Medical Research Council [grant number MR/Y010620/1].

M. Gaitán-Padilla, M. J. Pontes, M. E. V. Segatto, and C. A. R. Diaz are with the Telecommunications Laboratory (LabTel), Electrical Engineering Department, Federal University of Espírito Santo, Vitória; maria.padilla@edu.ufes.br; maria.pontes@ufes.br; marcelo.segatto@ufes.br; camilo.diaz@ufes.br.

M. Munera and C. Cifuentes are with the Bristol Robotics Laboratory, University of the West of England, Bristol, UK; marcela.munera@uwe.ac.uk; carlos.cifuentes@uwe.ac.uk.

pivotal sensor is photoplethysmography (PPG), which detects blood volume changes through optical methods, offering a non-invasive means to assess cardiovascular parameters [5]. Integrating these sensors, often in wearable or non-intrusive forms, enables a holistic approach to stress estimation [10].

Non-invasive and wearable sensors offer a continuous monitoring solution in various contexts [11], [12]. Often in wearable devices, optical sensors utilize light-based techniques such as PPG to assess physiological parameters, commonly found in wristbands and smartwatches, using light absorption and reflection to detect blood volume changes, providing heart rate measurements [5]. These devices facilitate real-time monitoring without impeding daily activities, enabling long-term data collection for robust assessments [5]. Furthermore, the integration of optical fiber sensors has expanded the capabilities of optical technology in physiological measurement. Optical fibers can be embedded in clothing [13], are highly sensitive [14], and have electromagnetic immunity [15]. Optical sensors have been used to measure medical biosignals, especially the FBG-based sensors, measuring biomechanical parameters, minimally invasive surgery applications and physiological monitoring [16]. In this sense, the sensors in the development process are classified according to the Technology Readiness Level (TRL), which describes the status where the advancement of the sensors and devices are currently [16].

The optical sensors' comfort and unobtrusiveness expand the research toward optimized and personalized health monitoring systems [17]. FBG-based optical sensors have been used for medical applications, in its pure and doped material for faster responses and detections [18]. In this case, the FBGs sensors are useful in multimodal pulse and respiratory rate monitoring applications [19], [20]. Nevertheless, their widespread adoption has been limited by the necessity for costly interrogation systems [21]. To address this limitation, various studies have endeavored to minimize the size and expense of those methods [22]. Moreover, some interesting approaches using FBG sensors have reported high-sensitive responses to these signals [18], and embedded in fabrics and printed designs to protect and achieve the measurement, leveraging the characteristics of size and weight of the optical fiber [13], [23]. *Zhichao et al.,* developed a system embedded in textiles containing three FBGs, one as the diaphragm, another for measuring heart rate, and the last one to measure breathing rate, and obtaining the peaks using the variational modal decomposition algorithm [23].

In this sense, *Lo Presti et al.,* developed a soft patch for simultaneously monitoring HR and RR through a single sensing device with a silicone cover and a textile with the bone form [13], achieving a correct measurement in supine, sitting, and standing positions in a protocol of eupnea and tachypnea. Similarly, *Presti et al.,* developed a dog-bone form sensor with an embedded FBG with a TPU 3D-printed encapsulation [20]. They made a metrological characterization and an analysis of the fiber in mechanical and thermal conditions, they tested the sensor in physiological measurement in a unique healthy volunteer during 60 seconds of normal breathing and 30 seconds of apnea, for which a larger quantity of volunteers is needed to see how the sensor measures different anatomical shapes and breathing patterns detection.

In addition, other structures have been designed with FBG sensors embedded, with different techniques, these optical fiber sensors are highly versatile to indirectly measure heart and respiratory rates [24]. In contrast, POF sensors have been an alternative approach for wearable sensors due to their size, resistant coating, and polymeric material [21]. POF sensors are easy to fabricate due to the detection method of light intensity and the facility for creating sensitive zones to generate variations [17]. The flexibility makes them more resistant to bend and handle, and are low-cost systems by using optoelectronic simple devices such as photodetectors and light emission diodes (LED) [25]. This generates the possibility of developing a stress-monitoring low-cost sensor. Stress estimation has had significant advancements with integrating machine learning (ML) techniques [8], offering a robust framework for analyzing physiological data. ML algorithms have demonstrated capabilities in discerning intricate patterns associated with stress [12]. These signals include HRV, electrodermal activity, and respiratory patterns by employing feature extraction methods and training [9]. *Lee et al.* [12] and *Castaldo et al.* [8] have successfully applied support vector machines (SVM), K-nearest neighbor (KNN), and ensemble methods to achieve accurate stress classification. The versatility of ML algorithms in handling diverse physiological datasets and their adaptability to real-time applications make them essential tools in developing stress estimation sensors [26].

This work seeks to validate a low-cost POF sensor for stress detection by monitoring pulse and respiration peaks and comparing it with another optical fiber sensor (FBG sensor) and a commercial ECG monitoring sensor (Shimmer Sensing, Ireland). To the authors' knowledge, this is the first reported approach of optical fiber sensors in stress estimation and comparing them with a reference sensor using ML algorithms. The proposed POF sensor seeks to improve well-being and give a low-cost solution for a daily-life world issue.

II. Materials and Methods

The methodology is based on comparing three physiological monitoring sensors for stress detection. This section describes the sensors' operation principle, the TSST protocol, experimental setup, signals obtained and its processing for feature extraction, and the ML classification process.

A. Used sensors' principle

This study used three sensors: a POF sensor based on light intensity variation, an FBG sensor based on wavelength light spectrum variation, and the commercial ECG monitoring sensor using electrical variation using electrodes.

1) POF sensor: The proposed POF sensor is made with a SH4001 Simplex Optical Fiber made of Polymethylmethacrylate (PMMA), with numerical aperture of 0.5, core and cladding of $\sim$980 and $\sim$1000 μm of diameter, and a Polyethylene jacket of $\sim$2200 μm (Mitsubishi Chemical Co., Japan). The sensor is based on the optical intensity variation concept, where a constant wavelength and intensity LED is connected through a POF to a photodetector configured with a trimmer to read as best as possible the light intensity variation [17]. The sensor has a light-sensitive area to generate

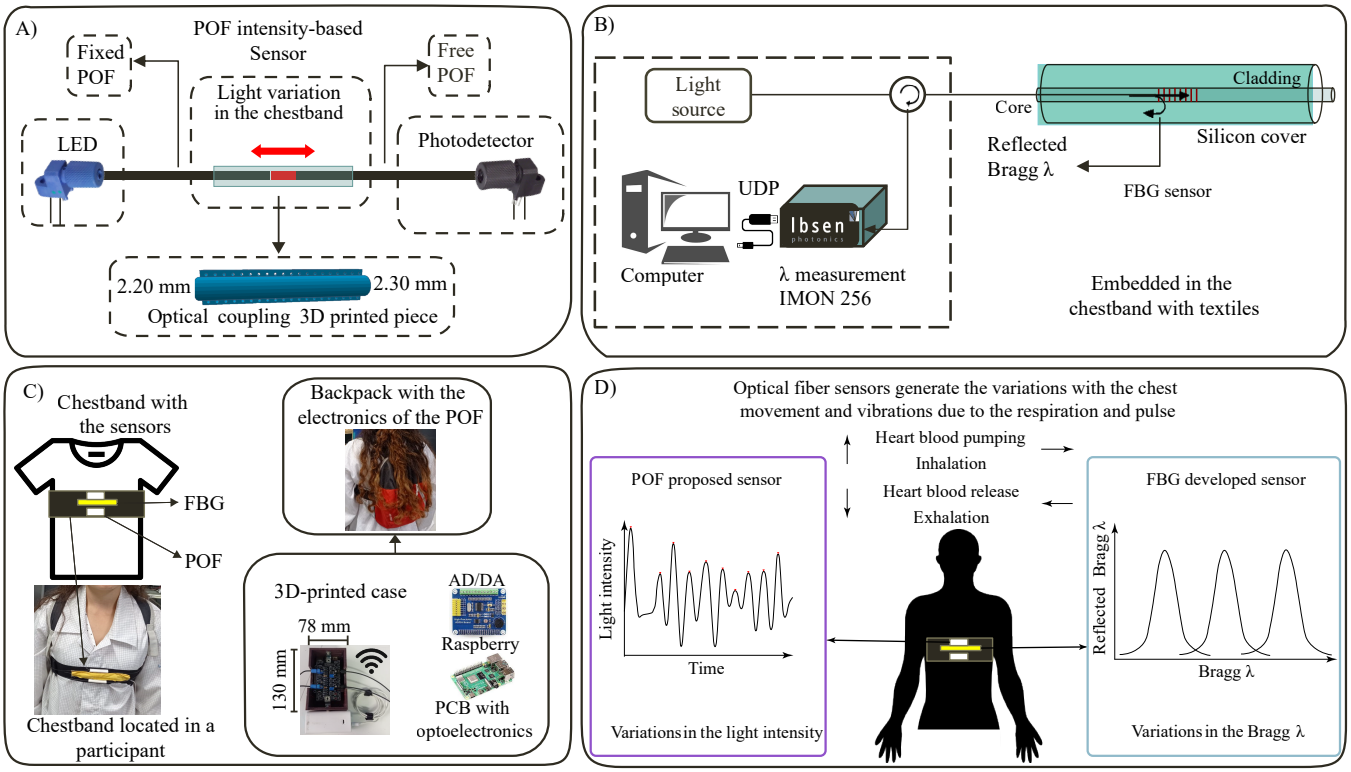

Fig. 1. Principle and functioning schematics of the sensors. A) The POF sensor intensity principle. B) The FBG sensor for physiological monitoring showing its principle and the division of the FBG in the chest band and the interrogation system. C) The chest band distribution and the backpack containing the electronics of the POF sensor. D) The variation of the optical fiber sensors according to the respiratory and pulse phases.

a variation in the light intensity that can be detected with a photodetector [27]. A 3D-printed piece was designed to maintain the coupling between two ends of POF, having one end fixed to the 3D-printed piece connected to the LED and another free-moving end connected to the photodetector; shown in Figure 1 (a).

This system located in the chest has a light loss depending on the expansion and contraction provoked by the pulse and the respiration as shown in Figure 1 (d), changing the distance between the POF ends inside the 3D-printed piece. Two of these light variation areas were distributed in an elastic velcro band to have redundant information and to be adaptable to subjects. An electronic circuit was designed, connecting the photodetectors and the LEDs to the High-Precision Analog to Digital and Digital to Analog (AD/DA) Board (Waveshare, United States) with 24-bit resolution. The AD/DA board was directly connected to a single board computer (SBC, Raspberry Pi4, United Kingdom), powered by a portable USB charger of 5V 2A (TP-Link, Brazil), as shown in the electronics segment of Figure 1 (c), showing the 3D printed case made for the electronics. The SBC stores and sends data through Wi-Fi by MQQT protocol to a computer with Matlab at 120 Hz. The electronics were stored in a small backpack.

2) FBG sensor: The FBG-based sensor was developed using a silica FBG centered at 1544.86 nm wavelength with 21 dB of extinction ratio, obtaining enough variation for this application [15]. To improve mechanical resistance, the FBG was protected with an elastic silicone coat of polydimethylsiloxane (PMDS) as used in other optical fiber sensor applications [28] and especially in FBG sensors to protect and give enough flexibility [13]. This allows the movement and variation of the FBG and makes it more robust for wearable use. The sensor was added to the elastic chest band in the middle of both POF coupling pieces, as shown in Figure 1 (c).

The FBG was monitored with an I-MON 256 High-Speed Interrogation monitor (1525-1570 nm) (Ibsen, photonics, Denmark), recording the FBG sensor's spectrum. It was connected to a broadband source centered at the C-band (DL-BP1-150A SLED, Denselight, Singapur) containing an internal optical circulator. The interrogator monitors the backscattered spectrum and the output Bragg wavelength spectrum; the interrogator was connected to a computer with the software to monitor and save the data; the sensor's schematic is shown in Figure 1 (b) with the FBG sensor principle. Still, when it is located on the participant's chest, the grating period changes due to the respiratory and pulse expansion (red-shift) and contraction (blue-shift), so the reflected Bragg wavelength depends on the physiological signals (see Figure 1 (d)).

3) ECG sensor: The Shimmer 3 Consensys ECG sensor (Shimmer sensing, Ireland) can be utilized to monitor four channels of ECG, recording the pathway of electrical impulses through the heart muscle. The ECG can also be used to monitor respiratory signals by connecting the electrodes as informed by the Shimmer documentation and shown in Figure 2. The software allows real-time monitoring of the heart's electrical activity and respiration. The ECG sensors work with the heart's electrical activity, so the heart cycle contraction can be seen. It is used in clinical and different lead setups, depending on the clinical evaluation objective, comparing the electrode voltage between them.

B. Ethics committee and Participants

The Rehabilitation Center Club Leones Cruz del Sur scientific committee accepts the protocol presented in this work as the validation-of-the-sensor stage, and the LabTel laboratory agrees with the development of the study in the laboratory facilities. The study involved 12 subjects (seven females and five males, 24.6 $\pm$ 3.5 years old). All of them were postgraduate students; the only exclusion criteria were anxiety-influenced subjects with any psychologically reported disease or any recent overstress episode. All subjects signed the informed consent allowing participation, divulgation, and video recording. The obtained data is publicly available[1].

C. TSST stress induction protocol

For stress-related studies, there have been discussions on the methods used for stress induction [29]. Results indicate the intersubject variability to specific stressors or the physiological and mental response for different classified stressors [30], so selecting the stress induction method depends on the participants, considering the environment, or using daily life situations that can induce stress [5]. This selection is a challenging task as it has been seen that conditions vary between subjects and groups to produce stress, i.e., a stressful stimulus does not affect everyone equally, so their physiological response will depend on how much a stimulus affects the subject [30]. For this reason, standard tests have been developed to induce types of stress, such as the TSST, which uses two types of stressors, a social and a mental task [12].

The protocol started by explaining the five steps (instrumentation of the sensors, relaxation, social and mental stress-induction test, and removal of the sensors) and signing the informed consent. After that, the five steps started as follows:

1) ECG sensor: Place 5 electrodes on the subjects as in Figure 2, placing the elastic band with the ECG sensor underwear connected to the electrodes. Subsequently, the two signals (respiration and ECG) were checked.

2) FBG sensor: Carefully place the elastic band over the clothing on the subjects' chest. Subsequently, the subjects are asked to sit in front of the monitor, and the wavelength signal is verified in the I-MON software of the optical interrogator.

3) POF sensor: The backpack with the electronics was placed with the help of the researcher. The POF ends were placed on the same elastic band of the FBG in the coupling pieces sewn previously to the band, connecting the LED end to the fixed connection and the photodetector end to the free-motion connection. Subsequently, the data status is checked in Matlab and synchronized with the video and the three sensors.

4) Relaxation induction: The participant is asked to sit comfortably, and "headspace: relax your mind" is played as the relaxation phase in the front monitor. This interactive video stimulates breathing and a relaxing visualization for 5 minutes.

5) Induction of social stress: The TSST stress test was designed to simulate challenging situations, such as a job interview. Five questions were asked and lasted between 3 to 5 minutes per subject.

6) Mental stress induction: The TSST mental stress test was with questions with positive and negative sound and visual feedback, but without giving the solution in case of being incorrect; this test had 30 questions, and the participants must answer as many questions as possible in 5 minutes.

7) Removal of the sensors: The sensors were paused, the video was stopped, and the sensors were removed.

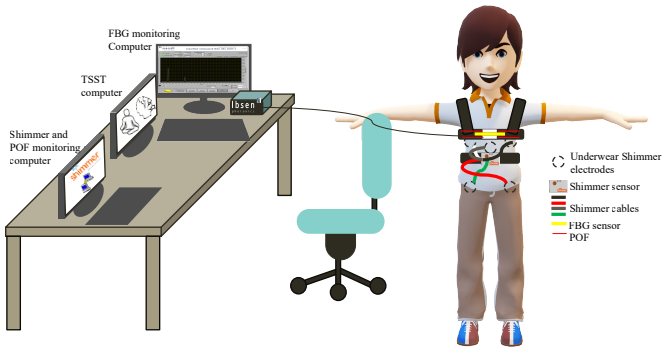

Fig. 2. Protocol setup on the laboratory facilities. The screens used for the sensors' software and the sensors located on the participant's chest.

D. Experimental setup

The experimental setup was planned to have a comfortable space to locate the sensors and conduct the protocol. In this study, our primary objective was to validate the sensor's ability to detect physiological signals under controlled conditions, rather than conducting a comprehensive metrological characterization. The experiments were performed in a temperature and humidity-controlled environment within a TTI lab (LabTel), ensuring that the sensor's performance was not influenced by variations in these environmental parameters. This approach was made focusing on the comparative validation of the sensor against reference sensors, it is worth noting those variables are slow dynamic and induce an optical power drift (dc offset) instead of a periodical amplitude modulation.

Optical fiber studies have investigated the influence of temperature and humidity on sensor performance, and have employed controlled environments to maintain consistent conditions. *Presti et al.,* analyzed temperature influences by exposing an FBG sensor to temperature changes of approximately 20 °C, followed by a static assessment as the temperature returned to ambient levels. Additionally, the effect of relative humidity (RH) was assessed by exposing the sensor to quasi-static RH changes, from 100% to approximately 20% [20]. The controlled environment in the current study ensures that the sensors' performance is reliable and not affected by environmental variations. A table was prepared with (1) a computer connected to the FBG interrogator and exclusively for the FBG monitoring due to its fragility and saving the data, (2) a second computer with the Shimmer Consensys software connected through Bluetooth to the sensor to monitor data acquisition and avoid disconnections, and the POF connection through SSH and Wifi, as *Betti et al.* who developed an interface to monitor sensors signals during TSST stress induction [31], and (3) a monitor connected to the second computer to display the TSST in front of the participant, as shown in Figure 2. A comfortable chair was arranged for the subjects, and the researcher stood near the second computer to manage the session flux, monitor the sensors' correct functioning, and make the protocol's social and mental stress questions.

[1]https://figshare.com/s/51cb5e18a6000ca550de

E. Features extraction for ML algorithms

Data processing and management are shown in Figure 4. This process is performed per sensor (i.e., feature matrices, training, and validations). The physiological validation was made to compare the results, with the detection of breathing and pulse peaks, and then, the stress classification with the performance of the ML algorithm validation. In addition, a test with the POF sensor data was conducted.

For data processing in the validation phase, each subject's first and last 30-second segments were omitted, and the relaxation and stress times were divided according to the video annotations. To confirm the frequency bands of the obtained signal with the POF, the first relaxation segment for each participant was analyzed, the raw data was plotted, and the fast Fourier transformation (FFT) was performed to see the frequency bands and confirm the filtering process. The frequency bands for the biosignals correspond to the normal frequencies of heart and respiratory rates, as have been defined previously [20], from 0.1 to 0.8 Hz for the respiration and from 1 to 3 Hz for the pulse. Comparing the 12 subjects' FFT with the bands found in the literature [23], [25], a Butterworth filter was implemented for each signal. After the filtering process, the signals were verified by plotting the signals obtained, this process is shown in Figure 3. After the filtering process, the Findpeaks function of Matlab was used to collect the peaks in both cases and for the three sensors.

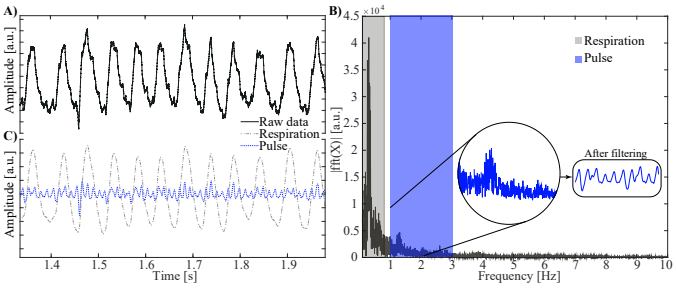

Fig. 3. The the POF sensor's filtering process. A) Raw and C) processed signals. B) FFT of the proposed sensor data with the two filtered sections highlighted and with zoom in the pulse peak.

Subsequently, 30-second windows are segmented, and a graphical comparison is performed as shown in Figure 5 for respiration and pulse. In this phase, the windows with disconnection lapses are discarded, thus obtaining 296 windows (120 in relaxation and 176 in stress). The peaks related to pulse and respiration are analyzed statistically between the sensors. The statistical Friedman test is performed to find significant differences in the number of peaks and the mean of the Standard Deviation (SD) of the peaks' intervals. Feature extraction uses pulse and respiration peaks to train and test different ML algorithms. The 24 pulse and respiration features listed in Table I are obtained for each time window, each participant, and each sensor. These features with a class flag, where 0 is relaxation, and 1 is stress, lead in three matrices of 296 rows and 25 columns.

The ECG and the FBG data are used 100% for training and validating, and the POF data are divided into 80% for training and validation and 20% for testing, as shown in Figure 4. For the feature selection method for classification applications, it

TABLE I
FEATURES DESCRIPTION EXTRACTED FROM BIOSIGNALS WITH THE THREE SENSORS WITH THE REFERENCE NUMBER [6], [9], [11], [12]

Signal	Feature number	Description
Pulse/Resp	(1) (2)	The average value of the 30 seconds segment
Pulse/Resp	(3) (4)	The median value of the signal
Pulse/Resp	(5) (6)	SD of how much fluctuates the signal from the mean
Pulse/Resp	(7) (8)	Skewness measures the signal's asymmetrical spread about its mean value
Pulse/Resp	(9) (10)	Kurtosis measures the signal peakedness
Pulse	(11)	The related SD of successive RR interval differences (SDSD) as short-term variability
Pulse	(12)	SD1 measures short-term HRV and correlates with baroreflex sensitivity (BRS), which is the change in inter-beat interval
Pulse	(13)	SD2 measures short-and longterm HRV and is correlated with LF power and BRS
Pulse	(14)	The ratio of SD1/SD2 measures the unpredictability of the RR time series, is used to measure ANS balance
Pulse/Resp	(15) (16)	The RMS represents the average power
Pulse/Resp	(17) (18)	The mean of the inter-peak intervals
Pulse/Resp	(19) (20)	SD of the inter-peak intervals
Pulse/Resp	(21) (22)	Number of peaks in the segment multiplied by two to obtain the estimated number of peaks in one minute
Resp	(23)	The mean amplitude of the respiratory peaks
Resp	(24)	The SD of the respiratory peaks

is essential to consider the characteristics of the data and the tested classification algorithms and compare the performance of different methods. Additionally, ensemble methods or combinations of multiple feature selection techniques are explored to improve robustness [32]. For dimension reduction, two feature selection techniques are used: the Maximum Relevance Minimum Redundancy (MRMR) algorithm [33] and the Chi-squared (Chi2) test [34].

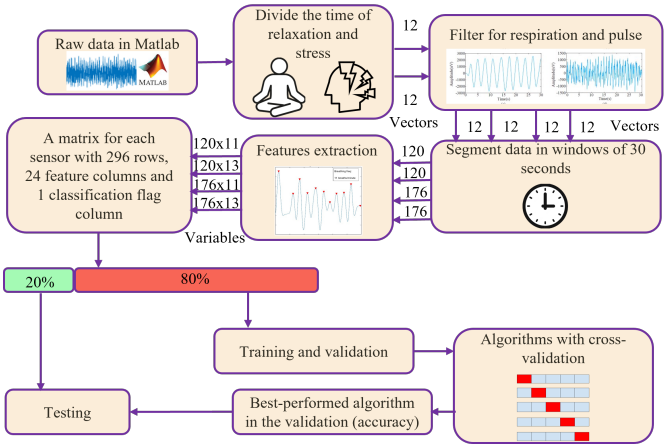

Fig. 4. Flux diagram for the features extraction and data flow for the stress classification algorithms.

Finally, the training and validation data are evaluated with the cross-validation technique with n=10, which divides the training data into ten equal parts. It performs algorithm training with nine parts and validates the algorithm with the remaining part. This procedure is performed to train an algorithm not influenced by overfitting. The main stress ML classification algorithms used in literature studies are tested (KNN [8], decision trees [9], and SVM [12] with and without feature reduction). For the POF, the best algorithm is used with

the test data. The test is carried out with 20 % of the POF data that have not yet encountered the algorithm. The four main evaluation metrics are obtained for the test: accuracy, precision, recall, and F-score.

III. Results and Discussion

This work validates the developed POF sensor using an FBG and an ECG as reference sensors. This results and discussion section includes the validation and comparison of the biosignals in the physiological measurement, the stress classification validation, and the test of the POF sensor for stress detection centered on evaluating the selected algorithm.

A. Physiological measurement validation

When performing feature extraction of the 30-second windows, a comparative difference analysis was performed to see if detecting the number of peaks and the mean time difference between them significantly differed between the sensors. This test would confirm that the signal peaks of the POF sensor corresponded to the heart and respiratory chest movements, by comparing with the reference sensors. A Shapiro-Wilk normality test was conducted to assess the normality of the data. Due to non-normal distribution, a comparative Friedman test was chosen as an appropriate non-parametric alternative. The results in Table II show the statistical comparison between the three sensors in four variables, the mean distance between pulse peaks, the standard deviation of the distance between pulse peaks, and the same for breathing. This indicates that all the calculated p-values exceed the alpha level of 0.05 for the sensor comparisons, and the results are not statistically different among the sensors in the pulse and respiration peak detections and peak-to-peak intervals. Additionally, a graphical analysis was made to see the differences in the measured signals among the three compared sensors. An example is shown in Figure 5, where the peak detection was correctly collected for both biosignals.

TABLE II
Friedman test between the three sensors in peak detection for pulse (1) and respiration (3) and peak-to-peak interval in pulse (2) and respiration (4)

Variable	POF	FBG	ECG	p-value
(1)	42.52 ± 15.11	45.81 ± 12.09	44.06 ± 16.53	0.32
(2)	0.70 ± 0.19	0.69 ± 0.20	0.63 ± 0.23	0.19
(3)	8.12 ± 2.01	8.52± 2.13	9.05 ± 1.85	0.40
(4)	3.10 ± 0.82	3.58 ± 0.49	3.25 ± 0.53	0.28

When evaluating the accuracy of physiological measurements, it is crucial to consider the context and intended use [35]. In this scenario, no significant difference was obtained in rest while comparing the wearable POF sensor, the FBG-based sensor, and an ECG device. Other studies showed mean absolute errors related to their reference of 1.6% in the heart rate and 0.78 breaths/minute in the respiratory rate by comparing with Masimo MightySat fingertip using the smartphone camera [35]. And percent differences of 0.6%, 0.9%, and 5.5% in the heart rate (HR) and non-errors in the respiratory rate with an FBG sensor compared with a Bioharness sensor [36].

The results in Figure 5 suggest that the wearable POF sensor may exhibit slight inaccuracies in measuring pulse and respiration rates, as in other studies of in-development sensors [37]. This margin of error is acceptable for specific applications and demonstrated by the lack of significant difference in comparing the main stress-related and independent variables extracted from the two measured physiological signals. In addition, Figure 5 (B) shows the heart activity's R peaks (pulse). *Haseda et al.* [38] discuss the importance of the waveshape for physiological heart measurement with optical fiber sensors; moreover, the application, in this case, extracts variables related to the detection of the R peaks for which the exact waveform is not necessary. Nevertheless, this limits the healthcare applications of the sensor for those based on superficial characteristics of the heart activity. Complete waveform sensors based on electrical heart activity are needed in scenarios where are required precise and accurate data and variables. FBG sensors have been used for more specific heart variable measurements, such as the blood pressure curve [38], where more complex heart variables can be extracted. Also, some novel approaches with doped FBG sensors made more sensitive sensors, which get to better detections and potential wearable applications in healthcare [18]. For this reason, an improved preprocessing must be done to obtain a more detailed biosignal waveform with the proposed POF sensor, as the Pan-Tompkins algorithm [39], and could be done by replicating the processing methods with the FBG signal [38]. Moreover, for this approach, simpler preprocessing was useful to obtain the respiratory and pulse peaks.

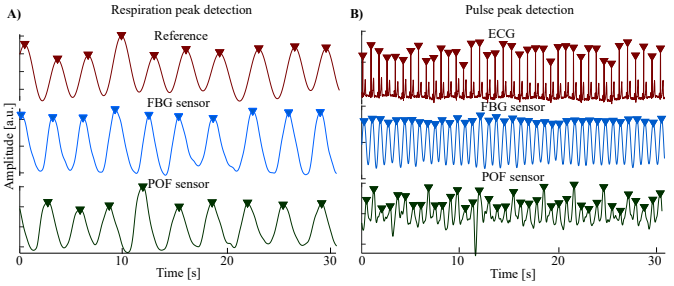

Fig. 5. Physiological signal from the ECG reference sensor, the FBG-based sensor, and the proposed POF sensor in the same 30-second interval A) Respiration and B) Pulse peaks detection.

The main reason to develop an intensity-based optical fiber sensor is the interrogation system needed in the FBG sensors. The FBG sensor used as the optical fiber sensor reference uses a costly and complex interrogation system, as in most of the developed FBG sensors for physiological measurement [13], [23], that measures the spectral response of FBGs to read the sensed data. This is a limitation for developing a wearable physiological sensor. Due to this complex equipment, the setups for FBG reading technologies are static [21]. *Shi et al.* developed a wearable FBG sensor for simultaneous sensing of respiration and heart rates, moreover while the sensing part is wearable in a chestband, the system needed a commercial interrogator with a size of 206 mm x 274 mm x 79 mm and highly costly compared to simpler optoelectronic elements like phototransistors, limiting the progress of the system for real wearable needed applications and accessible technology [24]. The FBG sensor showed a good performance during this work, and considering the recent interrogator's development field, as future work, a low-cost interrogation system could be tested

with the physiological monitoring system.

In the case of the proposed sensor and the evaluated setup, the measurements obtained may not be suitable for medical diagnoses or critical healthcare decisions. Still, in the case of monitoring full-day stress detection, the sensor provides a correct measurement being the first approach of a POF intensity-based sensor in stress detection, and with a 3D printed case with a size of 130 mm x 78 mm x 50 mm for the electronics and interrogation system, reducing the size and weight making the sensor a potential system for real-life scenarios measurement. The TRL of the developed sensor system is currently positioned at the third stage of proof of concept in the preliminary validation. Our focus in this study was primarily on demonstrating the sensor's functionality and comparing its performance against established reference sensors in the literature. While our system represents a foundational implementation, future efforts will be directed toward advancing its TRL through iterative development and testing. This will involve improving the sensor design, enhancing its integration into wearable devices, and conducting comprehensive validation studies to assess reliability and durability. By progressing through the TRL stages, is aimed to achieve the transition of the proposed sensor toward practical deployment and integration into wearable applications.

Also, while the current study focused on validating the sensor's ability to detect physiological signals, it is recognized the importance of understanding the sensor's behavior under varying environmental conditions for broader applications. Future studies will include comprehensive testing of the sensor's response to different temperature and humidity levels. This will involve placing the sensor in controlled environments where temperature and humidity can be systematically varied and monitored, similar to methodologies described in the literature [20]. These additional tests will allow the characterization of the sensor's metrological properties, including its sensitivity and response time to environmental changes, also approximating to real-world conditions.

Considering the context and intended use of the sensor, the POF sensor is portable, low-cost, and provides an acceptable measurement of pulse and respiratory signals. The wearable optical sensor was designed for monitoring applications; other optical sensors have been developed for fitness [40], monitoring [41], and users' individual use [30]. Their convenience and non-invasiveness make them well-suited for daily health and wellness tracking [15]. Moreover, clinical sensors are typically less suitable for long-term and continuous use outside of clinical environments [21]. This makes them less practical for full-day stress monitoring in everyday settings.

B. Stress cross-validation for the sensors comparison

With the matrices obtained, three training-with-cross-validation algorithms (KNN, BDTC, SVM) were tested with and without feature reduction. Two methods were implemented for a robust selection [32], and are shown in Figure 6, where the features referenced in Table I were ordered by importance scores. The MRMR algorithm, which minimizes redundancy [33], and the Chi-squared method to assess the independence between the variables [34]. A general score depending on the feature importance position was assigned and the variables were ordered from lower to higher, the features with a score lower than 12 were selected for the optimized training and validation test.

The chosen features were (11), (5), (9), and (13), all of them extracted from the pulse signal. The higher importance score for both methods, with a general score of 2, was the SDSD parameter, which indicates the related standard deviation of successive RR interval differences [6]. This is an HRV metric, but it is only related to short-term variability and is highly correlated to stress and ANS response [6], [8]. The standard deviation in time of the pulse signal was the second selected feature in the third position for both methods, with a general score of 6. This metric is not related to HRV but gives information on the signal variation along the segment [42]. The third selected metric was the pulse signal kurtosis, in the fourth position in the MRMR algorithm and the fifth position in the Chi-squared technique, with a general score of 9. Kurtosis represents a numerical value to the graphical behavior of the peakedness of the segment's signal [43]. Finally, the fourth feature selected was the SD2, sixth in both methods, with a general score of 12. This metric is related to the HRV as a non-linear measurement obtained from the Poincaré plot of the RR peaks intervals, representing short- and long-term HRV and correlates with Low Frequency (LF) power and BRS [6]. This variable is correlated to the body's stress response by representing LF variations and sympathetic activity [12].

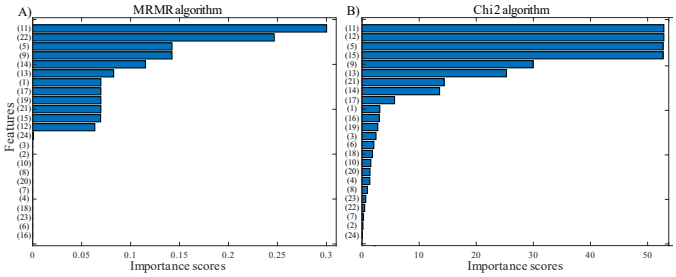

Fig. 6. Importance scores of the features reduction methods used. A) MRMR algorithm, and B) Chi2 statistical technique.

C. POF best-algorithm test evaluation metrics

The best algorithm was obtained while considering all the features of the three sensors. The POF sensor, combined with the BDTC algorithm (accuracy of 92.37%). For the FBG and ECG sensors, the KNN was the best performed during the cross-validation (accuracies of 94.93% and 95.61%). These results suggest that the sensors are highly effective in accurately classifying the data with stress-related variables. Furthermore, the accuracy results for all the tested algorithms in both situations are shown in Table III, comparing the results after the feature reduction.

TABLE III
ACCURACY RESULTS FOR THE THREE ALGORITHMS TESTED FOR THE THREE SENSORS WITH AND WITHOUT FEATURES REDUCTION

Sensor	All-features (%)			Features reduction (%)		
	KNN	BDTC	SVM	KNN	BDTC	SVM
ECG	**95.61**	88.55	91.58	90.65	87.42	89.10
FBG	**94.93**	89.63	90.27	91.50	83.31	85.69
POF	83.10	**92.37**	82.63	82.21	80.14	85.24

TABLE IV
RESULTS COMPARISON WITH OTHER RELATED STUDIES INCLUDING ML ALGORITHMS FOR STRESS CLASSIFICATION

Sensor	Results	Limitations
Proposed POF sensor	A comparison with ECG and FBG sensors for stress-related features with a low-cost POF sensor obtaining validation accuracy of 92.37% and test accuracy of 84.75% and precision of 93.10%	Waveform for other physiological applications, established and constant time windows
Multisignals approach with the Microsoft band [11]	Extreme gradient Boosting classifier with accuracy of 67.66% with multiphysiological information for mental load classification	Public dataset with previously reported low accuracies in the classification with dynamic sampling rates of HR and RR peaks and by using a commercial high-cost device
Polar H10 HR [12]	SVM algorithm tested in classification of police stress using short and ultra short HRV features with accuracies of 86.5% and 90.5%	Processing time, computing cost for real-time detection, waveform for other application and high-cost sensor
Multisignals approach with Bitalino [9]	Classification accuracy of 89.9% with a BDTC after a features reduction in anxiety-influenced participants (arachnophobia)	Classification algorithm for high stress for phobias therapy but low/middle stress differentiation could not be detected
Multisignals approach with the Empatica sensor [5]	Online approach using context identification algorithm for 55 days in real-life setups with five subjects with a precision of 95% and recall of 70%. With context the F1-score went from 0.47 to 0.90	Detection every 2 minutes, noisy blood pressure signal while moving, offline the high-stress detection was low, the tests were with low variety of subjects (5 subjects, all men, 28 years)
ECG sensor [8]	KNN algorithm used for stress classification with an accuracy of 94% in the validation and 88% in the test with feature reduction	Only mental stress task was used for the classification and use a low quantity of test data

The choice of classification algorithm plays a crucial role in achieving high accuracy [9]. In this case, the KNN algorithm and BDTC algorithm proved effective in classifying the sensors' data. It is essential to validate these results in real-world scenarios and consider factors such as sensor durability, ease of deployment, and data processing [5]. When evaluating stress monitoring solutions, it is crucial to consider accuracy and affordability [44], where POF sensors are generally more cost-effective than FBGs and ECG clinical devices [45]. Their affordability, coupled with the results obtained, makes them an attractive option for individuals seeking stress monitoring.

The best result with the cross-validation was with a BDTC, where the evaluation metrics with the test data were calculated. The 84.75% of accuracy obtained indicates that the POF sensor, when coupled with the BDTC algorithm, performed well in classifying stress and non-stress data. Precision measures the proportion of correctly identified stress cases among all positive predictions, and a 93.10% means that when the POF sensor predicts a case as stress, it is highly likely to be accurate. The 79.41% recall obtained indicates that the POF sensor captures a significant portion of stress cases. The F1 score was 85.71%, suggesting a good balance between accurately identifying stress cases and minimum false positives.

In the comparison in Table IV, other sensors and techniques reported similar results and accuracies. Initially, the proposed POF sensor is the first optical fiber sensor known by the authors to be used in stress estimation. Moreover, some limitations include indirect measurement, which generates difficulties in obtaining the complete heart waveform for other applications. *Lee et al.* applied traditional short HRV features and a novel ultrashort HRV feature to estimate police officers' stress with an accuracy of 86.5% and 90.5%, respectively. Their main limitations are the processing time and the cost of the sensor [12]. *Ihmig et al.* obtained an accuracy of 89.9% with their public database of spider-fearful subjects and the best results with a BDTC. However, the participants responded highly to the stress method, for which the algorithm with not fearful people may not work [9].

A classification system uses the context variable in real-time setups identification, with 95% precision. Moreover, the detection is made in real setups but every 2 minutes, which leads to stress periods that are not detected, and there is a noisy signal during some movements. Compared with reported fiber optic sensors, a detection analysis was found with the pulse through HRV features analysis with two participants [15], where the influence of stress was observed. However, no classification was performed. There are studies where the importance of separating subjects in extracting and analyzing features has been stated [11], which can be considered for an intersubject analysis study with the proposed sensor. Physiological responses to stress can vary widely among individuals, making it challenging to establish stress thresholds [5]. Moreover, the reported metrics should be considered when contemplating such variability. An accuracy of 84.75% indicates that the sensor and algorithm combination can effectively capture a substantial part of this variability, but some individuals may still exhibit atypical responses. The precision of 93.10% suggests that the sensor has minimized false positives caused by artifacts. In addition, environmental factors, sensor placement, and motion artifacts can introduce noise and affect accuracy [5]. For this, validation in no-controlled environments must be made, and efforts to improve data processing methods are needed [46].

IV. CONCLUSIONS

A POF sensor was developed and evaluated by comparing it with reference sensors in physiological detection and stress classification. The sensor employed a simple system using optical intensity detection; the results in the comparison show the sensor measuring the peaks of pulse and respiration as the FBG and the ECG sensors. The cross-validation results show that the ECG data had the best accuracy of 95.61%. The FBG and the POF also had optimal results of 94.93% and 92.37%, respectively. The test of the POF sensor shows acceptable results, mainly in its precision of 93.10%, and when compared with a developed FBG sensor.

For stress estimation in real setups, the no-significant difference in the physiological measurement shows the potential use of low-cost POF sensors in monitoring wearable devices, instead of FBG sensors, reducing costs and leveraging the advantages of using optical fiber in sensing applications. This study lays the groundwork for future advancements in wearable sensor technology using POF, and even when optical

fiber sensors have been used for physiological monitoring, to the knowledge of the authors, this is the first approach of POF and FBG sensors in stress estimation using ML algorithms.

The next step will involve a dedicated wearable system incorporating the sensor. This will include optimizing the sensor's form, exploring integration into soft and flexible materials, and leveraging additive manufacturing techniques for a lower-size customized 3D-printed case to advance in the TRL stages. Also testing the sensor and algorithm in real-world and online settings to validate the practical utility in stress monitoring applications outside controlled environments. Future research can explore strategies to address inter-subject variability, such as personalizing stress classification models to individual baseline physiological characteristics. Further efforts to enhance noise reduction and artifact handling techniques can improve sensor performance, especially in real-world, noisy environments.

REFERENCES

[1] J. E. Epping-Jordan *et al.*, "Self-help plus: A new who stress management package," *World Psychiatry*, vol. 15, no. 3, 2016.

[2] M. H. Foundation, *Stress: Statistics*, Accessed on October 15, 2023, 2018.

[3] M. Ising and F. Holsboer, "Genetics of stress response and stress-related disorders," *Dialogues in clinical neuroscience*, 2022.

[4] P. J. Brantley and G. N. Jones, "Daily stress and stress-related disorders," *Annals of behavioral medicine*, vol. 15, no. 1, 1993.

[5] M. Gjoreski *et al.*, "Monitoring stress with a wrist device using context," *Journal of biomedical informatics*, vol. 73, 2017.

[6] F. Shaffer and J. P. Ginsberg, "An overview of heart rate variability metrics and norms," *Frontiers in public health*, 2017.

[7] A. P. Allen *et al.*, "Biological and psychological markers of stress in humans: Focus on the trier social stress test," *Neuroscience & biobehavioral reviews*, vol. 38, 2014.

[8] R. Castaldo *et al.*, "Ultra-short term HRV features as surrogates of short term HRV: A case study on mental stress detection in real life," *BMC medical informatics and decision making*, vol. 19, no. 1, 2019.

[9] F. R. Ihmig *et al.*, "On-line anxiety level detection from biosignals: Machine learning based on a randomized controlled trial with spider-fearful individuals," *Plos one*, vol. 15, no. 6, 2020.

[10] X. Zhang *et al.*, "Recent progress of optical imaging approaches for noncontact physiological signal measurement: A review," *Advanced Intelligent Systems*, 2023.

[11] J. Tervonen *et al.*, "Ultra-short window length and feature importance analysis for cognitive load detection from wearable sensors," *Electronics*, vol. 10, no. 5, 2021.

[12] S. Lee *et al.*, "Mental stress assessment using ultra short term HRV analysis based on non-linear method," *Biosensors*, vol. 12, no. 7, 2022.

[13] D. Lo Presti *et al.*, "A soft and skin-interfaced smart patch based on fiber optics for cardiorespiratory monitoring," *Biosensors*, vol. 12, no. 6, p. 363, 2022.

[14] D. Lo Presti *et al.*, "A multi-point heart rate monitoring using a soft wearable system based on fiber optic technology," *Scientific reports*, vol. 11, no. 1, 2021.

[15] S. Koyama *et al.*, "Stress loading detection method using the FBG sensor for smart textile," *Journal of Fiber Science and Technology*, vol. 73, no. 11, 2017.

[16] D. L. Presti *et al.*, "Fiber bragg gratings for medical applications and future challenges: A review," *Ieee Access*, vol. 8, pp. 156 863–156 888, 2020.

[17] A. G. Leal-Junior *et al.*, "Polymer optical fiber sensors in healthcare applications: A comprehensive review," *Sensors*, vol. 19, no. 14, 2019.

[18] J. Bonefacino *et al.*, "Ultra-fast polymer optical fibre bragg grating inscription for medical devices," *Light: Science & Applications*, vol. 7, no. 3, pp. 17 161–17 161, 2018.

[19] L. Zhichao *et al.*, "Heartbeat and respiration monitoring based on FBG sensor network," *Optical Fiber Technology*, vol. 81, 2023.

[20] D. L. Presti *et al.*, "Optimization and characterization of a 3d-printed wearable strain sensor for respiration and heartbeat measurements," *Measurement*, p. 114 377, 2024.

[21] C. Broadway *et al.*, "Toward commercial polymer fiber bragg grating sensors: Review and applications," *Journal of Lightwave Technology*, vol. 37, no. 11, 2019.

[22] C. A. R. Diaz *et al.*, "Perrogator: A portable energy-efficient interrogator for dynamic monitoring of wavelength-based sensors in wearable applications," *Sensors*, vol. 19, no. 13, 2019.

[23] L. Zhichao *et al.*, "Heartbeat and respiration monitoring based on fbg sensor network," *Optical Fiber Technology*, vol. 81, p. 103 561, 2023.

[24] C. Shi *et al.*, "Development of an fbg-based wearable sensor for simultaneous respiration and heartbeat measurement," *IEEE Transactions on Instrumentation and Measurement*, vol. 72, pp. 1–9, 2022.

[25] A. G. Leal-Junior *et al.*, "Polymer optical fiber-based sensor for simultaneous measurement of breath and heart rate under dynamic movements," *Optics & Laser Technology*, vol. 109, 2019.

[26] A. R. Raju *et al.*, "Galvanic skin response based stress detection system using machine learning and IoT," in *2th International Conference on Augmented Intelligence and Sustainable Systems*, IEEE, 2023.

[27] J. Casas *et al.*, "Large-range polymer optical-fiber strain-gauge sensor for elastic tendons in wearable assistive robots," *Materials*, vol. 12, no. 9, 2019.

[28] L. De Arco *et al.*, "Soft-sensor system for grasp type recognition in underactuated hand prostheses," *Sensors*, vol. 23, no. 7, 2023.

[29] R. Ahuja *et al.*, "Mental stress detection in university students using machine learning algorithms," *Procedia Computer Science*, vol. 152, 2019.

[30] K. Nkurikiyeyezu *et al.*, "The effect of person-specific biometrics in improving generic stress predictive models," *arXiv preprint arXiv:1910.01770*, 2019.

[31] S. Betti *et al.*, "Evaluation of an integrated system of wearable physiological sensors for stress monitoring in working environments by using biological markers," *IEEE Transactions on Biomedical Engineering*, vol. 65, no. 8, 2017.

[32] T. Iqbal *et al.*, "Improved stress classification using automatic feature selection from heart rate and respiratory rate time signals," *Applied Sciences*, vol. 13, no. 5, 2023.

[33] I. K. Ihianle *et al.*, "Minimising redundancy, maximising relevance: HRV feature selection for stress classification," *Expert Systems with Applications*, 2023.

[34] P. Tiwari *et al.*, "An efficient classification technique for automatic identification of emotions leading to stress," in *6th Conference on Information and Communication Technology*, IEEE, 2022.

[35] S. Bae *et al.*, "Prospective validation of smartphone-based heart rate and respiratory rate measurement algorithms," *Communications medicine*, vol. 2, no. 1, 2022.

[36] C. Tavares *et al.*, "Respiratory and heart rate monitoring using an FBG 3d-printed wearable system," *Biomedical Optics Express*, vol. 13, no. 4, 2022.

[37] J.-H. Park *et al.*, "Wearable sensing of In-Ear pressure for heart rate monitoring with a piezoelectric sensor," *Sensors*, vol. 15, no. 9, 2015.

[38] Y. Haseda *et al.*, "Measurement of pulse wave signals and blood pressure by a plastic optical fiber FBG sensor," *Sensors*, vol. 19, no. 23, 2019.

[39] M. Fariha *et al.*, "Analysis of pan-tompkins algorithm performance with noisy ecg signals," in *Journal of Physics: Conference Series*, IOP Publishing, vol. 1532, 2020, p. 012 022.

[40] B. Bent *et al.*, "Investigating sources of inaccuracy in wearable optical heart rate sensors," *NPJ digital medicine*, vol. 3, no. 1, 2020.

[41] M. Namvari *et al.*, "Photoplethysmography enabled wearable devices and stress detection: A scoping review," *Journal of Personalized Medicine*, vol. 12, no. 11, 2022.

[42] Z. Fan *et al.*, "Pulse wave analysis," in *Advanced Biomedical Engineering*, IntechOpen, 2011.

[43] J.-Q. Li *et al.*, "Design of a continuous blood pressure measurement system based on pulse wave and ECG signals," *IEEE journal of translational engineering in health and medicine*, vol. 6, 2018.

[44] N. E. J. Asha, R. Khan, *et al.*, "Low-cost heart rate sensor and mental stress detection using machine learning," in *5th International Conference on Trends in Electronics and Informatics*, IEEE, 2021.

[45] K. Ogawa *et al.*, "Wireless, portable fiber bragg grating interrogation system employing optical edge filter," *Sensors*, vol. 19, no. 14, 2019.

[46] S. Prakash *et al.*, "A study on artifacts removal from physiological signals," in *6th International Conference on Signal Processing, Computing and Control*, IEEE, 2021.